

# Extended-Cavity Semiconductor Wavelength-Swept Laser for Biomedical Imaging

S. H. Yun, C. Boudoux, M. C. Pierce, J. F. de Boer, G. J. Tearney, and B. E. Bouma

**Abstract**—We demonstrate a compact high-power rapidly swept wavelength tunable laser source based on a semiconductor optical amplifier and an extended-cavity grating filter. The laser produces excellent output characteristics for biomedical imaging, exhibiting >4-mW average output power, <0.06-nm instantaneous linewidth, and >80-dB noise extinction with its center wavelength swept over 100 nm at 1310 nm at variable repetition rates up to 500 Hz.

**Index Terms**—Optical coherence tomography (OCT), semiconductor lasers, tunable lasers.

**R**APIDLY tuning wavelength-swept lasers [1]–[7] have great potential as optical sources for biomedical imaging such as optical coherence tomography (OCT) and spectrally encoded confocal microscope. Desirable output characteristics of wavelength-swept lasers include high power, fast repetition rate, narrow instantaneous linewidth, and broad wavelength tuning range. Although single-longitudinal-mode tuning can be achieved in an extended-cavity semiconductor laser using an elaborate grating filter configuration [8], the tuning speed demonstrated so far has been limited less than 0.1 nm/ms. For several biomedical applications, the single-frequency operation may not be essential and can be compromised to enhance tuning speed. Optical penetration in biological samples is limited by absorption and scattering but in general is optimized for wavelengths in the vicinity of 1.3  $\mu\text{m}$  [9]. For imaging modalities that limit detection primarily to singly scattered light, maximum depth of penetration is on the order of a few millimeters. For frequency domain OCT [5], [6], this depth corresponds to an instantaneous linewidth of an order of 10 GHz. Broad wavelength tuning is desirable since the depth resolution in OCT is inversely proportional to the tuning range. Narrow linewidth and broad tuning range are also important for spectrally encoded confocal microscopy [10] in order to achieve micron-level transverse resolution and wide field of view, respectively. In this letter, we demonstrate an extended-cavity semiconductor wavelength-swept laser that has many attractive

Manuscript received May 22, 2003; revised July 30, 2003. This work was supported in part by the National Science Foundation under Grant BES-0 086 709, CIMIT, and by a gift from Dr. and Mrs. J. S. Chen to the optical diagnostics program of the Massachusetts General Hospital Wellman Laboratories of Photomedicine.

S. H. Yun, M. C. Pierce, J. F. de Boer, G. J. Tearney, and B. E. Bouma are with the Harvard Medical School and Wellman Laboratories for Photomedicine, Massachusetts General Hospital, Boston, MA 02114 USA (e-mail: syun@bics.bwh.harvard.edu).

C. Boudoux is with the Harvard-MIT Division of Health Sciences and Technology and Department of Nuclear Engineering, Wellman Laboratories of Photomedicine, Massachusetts Institute of Technology, Boston, MA 02114 USA.

Digital Object Identifier 10.1109/LPT.2003.820096

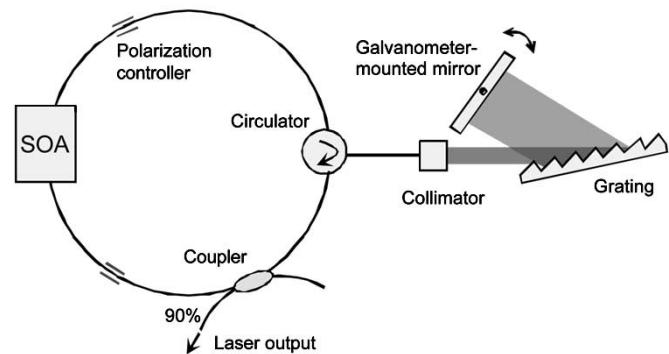


Fig. 1. Configuration of the tunable laser.

features for the biomedical imaging applications. The laser outperforms other tuning lasers previously demonstrated in that it simultaneously provides high power (10 mW) polarized light, narrow linewidth (10 GHz), broad wavelength tuning (100 nm centered at 1310 nm), and fast repetition rates (up to 500 Hz). Moreover, the compactness offered by using of a semiconductor gain medium makes the laser suitable for use in the clinical environment.

Fig. 1 shows the schematic of the laser. The semiconductor optical amplifier [(SOA) Philips CQF882/e] gain medium provided high saturation power and a broad spectrum around 1310 nm. Wavelength tuning is achieved by using a diffraction grating (1200 lines per millimeter, blazed reflective type) and a rotating mirror mounted on a fast galvanometer in the extended-cavity configuration. The double-pass Littman grating filter was configured to have a filtering bandwidth of 0.12 nm (21 GHz) at 1310 nm. The peak transmission (reflectivity) of the filter was approximately  $-6.5$  dB, independent of the tuning speed and direction, in the 1200–1400-nm wavelength range. The tuning range and repetition rate are controlled by the voltage and frequency of the drive signal to the linear-servo galvanometer. The galvanometer (Cambridge Tech.) could be operated up to 500 Hz with sufficient angular deflection for 100-nm wavelength tuning.

A ring-cavity geometry with an optical circulator for unidirectional operation was chosen to optimize output coupling and rejection of amplified spontaneous emission from the SOA. Due to polarization sensitivity of the grating filter and the SOA gain medium, we placed two polarization controllers in the cavity to align the polarization state to the axes of maximum transmission and gain. The laser output was obtained through a 90% fused coupler after the filter. The longitudinal-mode spacing was 27 MHz. The lasing threshold current for the SOA was

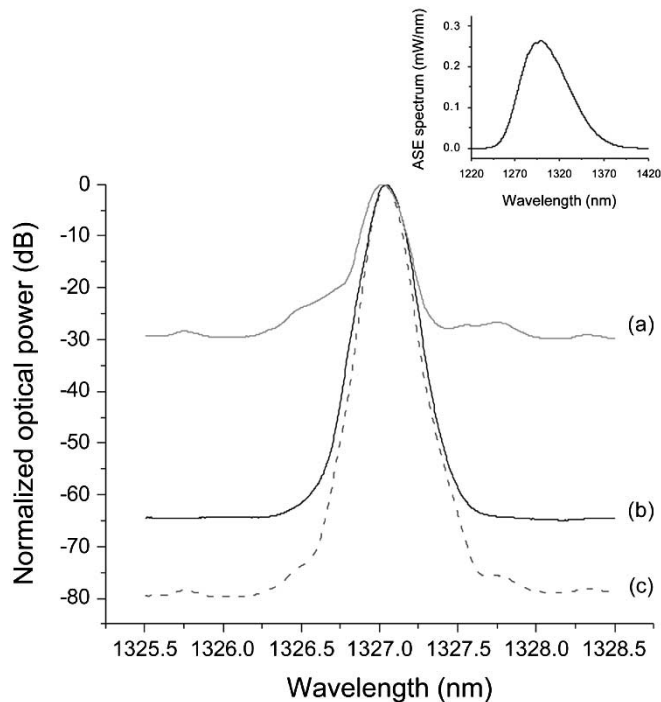


Fig. 2. (a) Normalized spectrum of filter profile. Laser output spectra (b) measured and (c) calculated. The inset is the amplified spontaneous emission spectrum from the SOA at injection current of 480 mA.

60 mA. All the experimental results presented here were obtained at an injection current of 480 mA, a maximum available from the current source that was used.

The laser produced polarized, single-transverse mode continuous-wave (CW) output. The linewidth of the laser emission was calculated from the coherence length of the output which was measured using a variable-delay Michelson interferometer. The measured linewidth was  $<0.06$  nm (10 GHz) at a wavelength sweep rate from 0 to 500 Hz. The instantaneous linewidth corresponds to a span of several hundreds of longitudinal modes. The multiple mode oscillation resulted in peaks in the electrical spectrum of a laser output, with typical magnitude of  $-65$  dB/Hz at harmonics frequencies of 27 MHz. In between the peaks, the relative intensity noise level was less than  $-127$  dB/Hz.

In order to understand the fundamental properties of the laser, performance was first investigated while maintaining the filter at a fixed wavelength. The curve in Fig. 2(a) is a typical profile of the filter fixed at 1327 nm, measured using amplified spontaneous emission light from the SOA (inset of Fig. 2). The curve in Fig. 2(b) is the output spectrum of the laser. Both spectra were obtained with an optical spectrum analyzer (resolution bandwidth of 0.1 nm) and normalized to their peak values. It is worth noting that the output spectrum has been shifted from the center of the filter profile toward a longer wavelength by approximately 0.045 nm (7.7 GHz). Further investigation suggested that the spectral offset resulted from self-frequency shift of the intracavity laser light in the SOA gain medium. The spectrum of the intracavity laser light continuously experiences a frequency downshift by as much as 4 GHz as it passes through the SOA. This effect caused the steady-state output spectrum to be centered at a position shifted away (toward a longer wavelength)

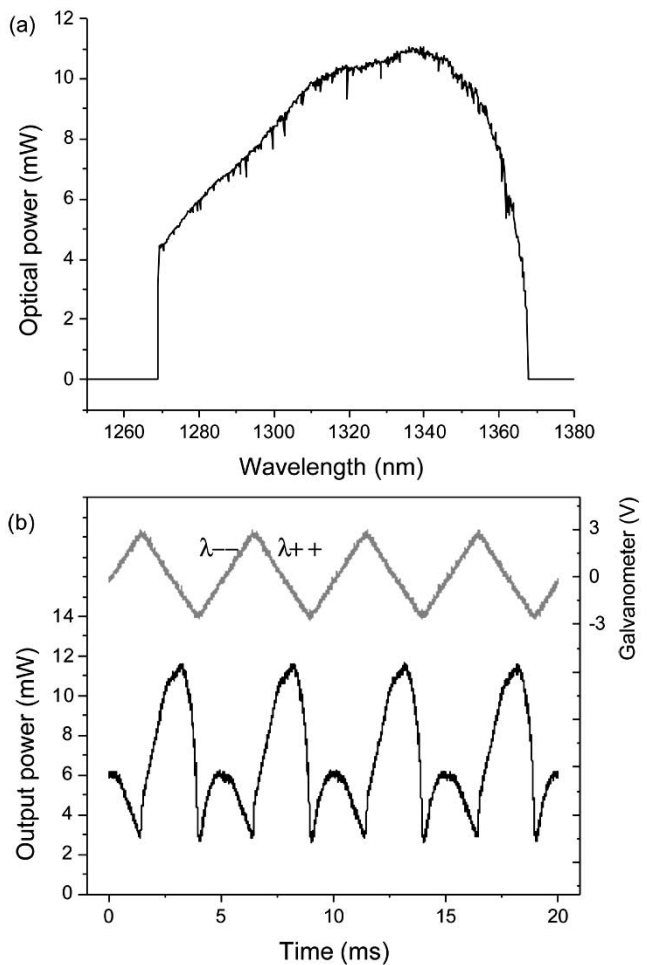


Fig. 3. (a) Peak-hold output spectrum and (b) time-domain laser output trace when the filter is scanned over 100 nm at 200 Hz.

from the center of the filter in the wavelength domain. The physical mechanism for the self-frequency shift is believed to be intraband four-wave mixing via the carrier-density modulation in the SOA [11], [12]. The optical spectrum analyzer we used had a power dynamic range of only 60 dB, not enough to measure the spontaneous emission noise level accurately. Therefore, we measured the spectrum of the laser light entering the filter by placing a 10% tap coupler immediately before the filter. The measured spectrum was multiplied by the measured filter profile [Fig. 2(a)] to estimate the output spectrum, which is shown in Fig. 2(c). The spontaneous emission noise level relative to the peak of the laser spectrum is about 80 dB. Such high extinction is highly desirable in optical imaging applications where the total noise power, integrated over the entire spectrum, should be substantially smaller than the total signal power within the narrowband spectrum.

Fig. 3(a) depicts the typical output spectrum measured in peak-hold mode of the optical spectrum analyzer, when the galvanometer was driven by a triangular waveform at 200 Hz. Because of the polarization sensitivity of the intracavity components and the birefringence in the fiber, the cavity exhibited weak wavelength-dependent loss. This effect could be used to tailor the overall shape of the spectrum in Fig. 3(a); by altering the settings of the polarization controllers, the shape could be made more Gaussian or more nearly flat. This shaping, however,

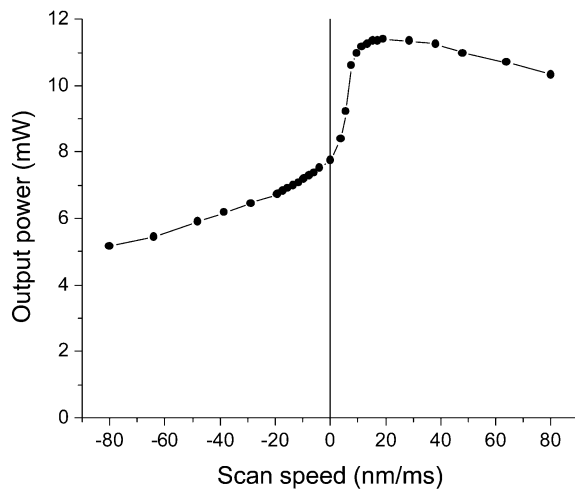


Fig. 4. Peak output power measured as a function of the scan speed.

also influences overall power output. Fig. 3(a) was acquired when the polarization controllers were adjusted for maximum average output power.

Fig. 3(b) shows the laser output in the time domain. The upper trace is the galvanometer position sensor voltage which is proportional to the negative of the filter wavelength. In this case, the wavelength is scanned alternately in positive (decreasing galvanometer voltage) and negative (increasing galvanometer voltage) linear wavelength sweeps. Although the interplay between a scanning filter and nonlinearity in an optical fiber cavity can lead to modelocked pulse formation [7], it is believed that the pulse broadening effect of fast gain saturation in the SOA was dominant and led to CW emission. The lower trace of Fig. 3(b) represents the laser output power while scanning. A two-fold increased power was observed during positive sweeps relative to negative sweeps. This power asymmetry is also attributed to the frequency downshift occurring in the SOA. When the filter profile is scanned in the same direction as the frequency shift, the spectral offset of the laser spectrum from the center of the filter is reduced, resulting in lower loss in the filter and increased output power.

To further characterize the laser, the peak emitted power during positive and negative sweeps was measured as a function of scan speed. Measurements were made while varying the scan frequency from 0 to 500 Hz at a constant sweep range of 80 nm and while varying the sweep range from 0 to 80 nm and holding the scan frequency fixed at 500 Hz. For these measurements, the polarization controllers were adjusted to give maximum output power at the center of the tuning range (1317 nm). Results for scan speeds ranging from dc to  $\pm 80$  nm/ms are shown in Fig. 4. If the frequency shift per cavity round trip were to be independent of tuning rate, we would expect the maximum

peak power in Fig. 4 to appear at 624 nm/ms (4-GHz shift per round trip) [4]. In the case of frequency shift arising from intraband four-wave mixing, we would expect the magnitude of the shift to depend on linewidth and therefore on scanning speed. As the scanning speed is increased toward resonance with the frequency shift, the linewidth would decrease resulting in a decreased shift. Although this explanation qualitatively agrees with the observed results, confirmation awaits a more thorough theoretical analysis.

In conclusion, we have demonstrated an extended-cavity wavelength-swept semiconductor laser optimized for application to biomedical imaging. The laser produced  $>4$ -mW average output power with an instantaneous linewidth of  $<0.06$  nm, and could be tuned over a wavelength range of 100 nm at a repetition rate of 500 Hz. The 80-dB optical signal-to-noise ratio of this laser is of particular importance for the detection of weak backreflections from within biological tissue.

#### REFERENCES

- [1] P. F. Wysocki, M. J. Digonnet, and B. Y. Kim, "Broad-spectrum, wavelength-swept, erbium-doped fiber laser at  $1.55 \mu\text{m}$ ," *Opt. Lett.*, vol. 15, pp. 879–881, 1990.
- [2] P. Zorabedian, "Tuning fidelity of acoustooptically controlled external-cavity semiconductor lasers," *J. Lightwave Technol.*, vol. 13, pp. 62–66, Jan. 1995.
- [3] K. Takada and H. Yamada, "Narrow-band light source with acoustooptic tunable filter for optical low-coherence reflectometry," *IEEE Photon. Technol. Lett.*, vol. 8, pp. 658–660, May 1996.
- [4] S. H. Yun, D. J. Richardson, D. O. Culverhouse, and B. Y. Kim, "Wavelength-swept fiber laser with frequency shifted feedback and resonantly swept intracavity acoustooptic tunable filter," *IEEE J. Select. Topics Quantum Electron.*, vol. 3, pp. 1087–1096, Aug. 1997.
- [5] S. R. Chinn, E. Swanson, and J. G. Fujimoto, "Optical coherence tomography using a frequency-tunable optical source," *Opt. Lett.*, vol. 22, pp. 340–342, 1997.
- [6] B. Golubovic, B. E. Bouma, G. J. Tearney, and J. G. Fujimoto, "Optical frequency-domain reflectometry using rapid wavelength tuning of a  $\text{Cr}^{4+}$ :forsterite laser," *Opt. Lett.*, vol. 22, pp. 1704–1706, 1997.
- [7] S. H. Yun, D. J. Richardson, and B. Y. Kim, "Interrogation of fiber grating sensor arrays with a wavelength-swept fiber laser," *Opt. Lett.*, vol. 23, pp. 843–845, 1998.
- [8] K. C. Harvey and C. J. Myatt, "External-cavity diode laser using a grazing-incidence diffraction grating," *Opt. Lett.*, vol. 16, pp. 910–912, 1991.
- [9] B. E. Bouma, G. J. Tearney, I. P. Bilinsky, B. Golubovic, and J. G. Fujimoto, "Self-phase-modulated Kerr-lens mode-locked Cr:forsterite laser source for optical coherence tomography," *Opt. Lett.*, vol. 21, pp. 1839–1841, 1996.
- [10] G. J. Tearney, R. H. Webb, and B. E. Bouma, "Spectrally encoded confocal microscopy," *Opt. Lett.*, vol. 23, pp. 1152–1154, 1998.
- [11] G. P. Agrawal, "Population pulsations and nondegenerate four-wave mixing in semiconductor lasers and amplifiers," *J. Opt. Soc. Amer. B*, vol. 5, pp. 147–159, 1988.
- [12] K. Inoue, T. Mukai, and T. Saitoh, "Nearly degenerate four-wave mixing in a traveling-wave semiconductor laser amplifier," *Appl. Phys. Lett.*, vol. 51, pp. 1051–1053, 1987.